論文 / 著書情報
Article / Book Information

Title	Measurement of Creep Deformation of Resin Structural Parts for a Lightweight Industrial Robot
Authors	Yuta Tsukamoto, Kenji Sekiguchi, Hiroyuki Nabae, Gen Endo
Citation	Proceedings of the 2024 IEEE/SICE International Symposium on System Integration, , , pp. 592-597
Pub. date	2024, 1
Copyright	(c) 2024 IEEE. Personal use of this material is permitted. Permission from IEEE must be obtained for all other uses, in any current or future media, including reprinting/republishing this material for advertising or promotional purposes, creating new collective works, for resale or redistribution to servers or lists, or reuse of any copyrighted component of this work in other works.
DOI	http://dx.doi.org/10.1109/SII58957.2024.10417463
Note	This file is author (final) version.

Measurement of Creep Deformation of Resin Structural Parts for a Lightweight Industrial Robot*

Yuta Tsukamoto[1], Kenji Sekiguchi[1], Hiroyuki Nabae[1], and Gen Endo[1]

Abstract— **Lightweight industrial robots are increasingly required to reduce power consumption. In this research, we focus on lightweight resin materials such as 3D printed parts, and our ultimate goal is to develop practical industrial robots using these materials as structural parts. Unlike conventional light metal materials such as high-strength aluminum, resin materials have creep deformation properties even at room temperature, which deteriorates the end-point position accuracy in practical use over a long period. In this paper, we fabricated an experiment apparatus that can measure creep deformation by applying 40 kgf of load at the end of a beam specimen. A laser displacement meter accurately measured the creep deformation for approximately two months (1600 hours). For comparison, we measured the creep deformation of six specimens of five different lightweight resin materials and conventional aluminum alloys (A5052). The results showed that 3D printed materials had large creep deformation, whereas A5052 and FELCARBO showed almost no creep deformation.**

I. INTRODUCTION

Industrie 4.0, has led to introduction of industrial robots to production lines to improve factory productivity. Reducing the energy consumption of industrial robots is a crucial goal for achieving sustainable development and reducing production costs. One of the most straightforward methods to reduce energy consumption is to reduce the weight of industrial robots. In particular, weight reduction in the structural parts of industrial robots can reduce the actuator power consumption in operation. Furthermore, the weight reduction in the structural parts is an effective method because it permits the robot to use a smaller actuator that eventually reduces the weight of the actuator and the total weight of the industrial robot. The authors' research group is conducting fundamental research to reduce the weight of conventional industrial robots by 25% by applying new lightweight materials for structural parts and reduction gears.

One of the essential design items for the structural parts of industrial robots includes durability against generated stress and vibration that occur during use. The generated stress and deformation should be predicted based on stress analysis, and the appropriate material and shape should be determined based on the design specifications, such as the workspace and payload capacity. Then, structural modifications based on vibration analysis are applied to avoid deterioration of controllability and damage due to resonance. There are many examples of research on structural optimization through design based on the above analysis [1][2].

However, this design method is applicable in the case of metal materials because the metal materials can be approximated by a linear material, and the stress and vibration analysis are sufficiently accurate. On the other hand, a resin material is a non-linear material. Moreover, its mechanical property also depends on the processing methods. For example, the mechanical properties of a resin specimen manufactured by machining process from bulk material would be different from a resin specimen manufactured by a 3D printing process, which is represented by the Fused Filament Fabrication (FFF) method, due to lamination modeling. Therefore, it is necessary to experimentally accumulate the fundamental mechanical properties of a resin material, considering a realistic use case.

In our previous works, we fabricated standard specimens with different materials that simplified the structural part of the link of an industrial robot and one degree-of-freedom experimental apparatus with a harmonic drive actuator unit. We measured vibration damping property with the specimens [4] and compared the stiffness of the specimens as a manipulator structure [5]. We also have proposed a new fastening method to connect the specimens to a rigid metal part [6].

In this paper, we particularly focus on the creep deformation of the specimens. It is generally known that resin materials gradually deform when a static load is applied for a long time, even at room temperature. This creep deformation changes the relative position and orientation of the joints of the manipulator and degrades the accuracy of the end-point position control. Therefore, measuring creep deformation is essential to evaluate the applicability of resin materials for an industrial robot.

Although many studies have been conducted on creep testing of standard specimens of materials such as ABS and PLA, commonly used for 3D printing [7][8]. However, the standard specimen is very small, and there is no guarantee that the result is scalable and directly applicable to the large-sized industrial robot. Therefore we assume a more realistic link length and load condition.

This paper aims to fabricate a large-scale experiment apparatus with laser displacement sensors and measure creep deformation when 40 kgf of the load is applied to the end of the specimen. The six specimens with different materials are measured simultaneously, and obtain creep deformation data for two months (67days, 1600 hours). We quantitatively compare and discuss the findings.

*This research is subsidized by New Energy and Industrial Technology Development Organization (NEDO) under a project JPNP20016.

[1]All authors are with the Department of Mechanical Engineering, Tokyo Institute of Technology, 2-12-1 Ookayama, Meguro-ku, Tokyo 152-8550, Japan, {tsukamoto.y.ak, sekiguchi.k.ai, nabae.h.aa, endo.g.aa}@m.titech.ac.jp

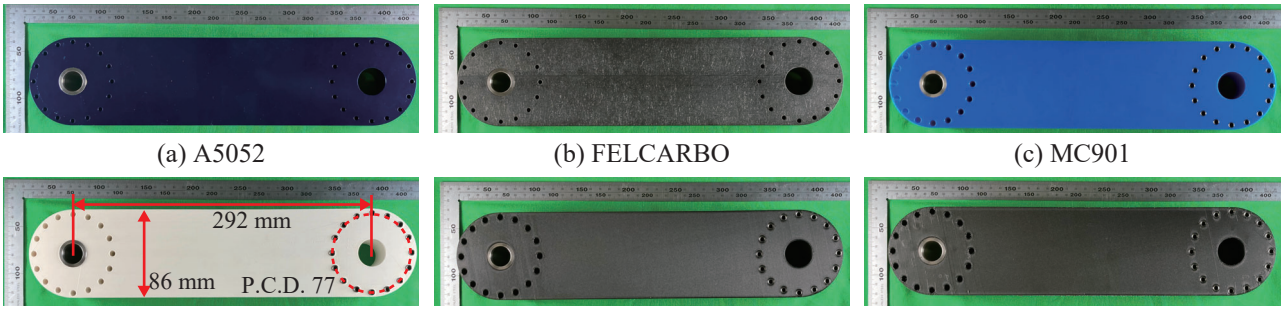

(a) A5052 (b) FELCARBO (c) MC901

(d) POTICON (e) Onyx (f) Onyx+CF

Fig. 1: Shape of the specimen. (a) A5052 is the aluminum alloy. (b) FELCARBO and (c) MC901 are resin parts machined from bulk material. (d) Onyx, (e) Onyx + CF, and (f) POTICON are 3D printed parts.

TABLE I: Weight of links (the metal sleeves for connection shown in Fig. 1 are not included).

Link	Material	Mass [g]	Processing method	Cost [yen]
1	A5052	3531.8	Machining	19,640
2	FELCARBO	1756.1	Machining	57,660
3	MC901	1502.5	Machining	14,300
4	POTICON	658.4	3D printing	51,355
5	Onyx	609.3	3D printing	30,000
6	Onyx+CF	646.0	3D printing	31,900

II. Specimens

The specimens are shown in Fig. 1 and their masses, processing methods and costs are indicated in Table I. A specimen is fabricated for each of the following six materials: an aluminum alloy (A5052), which is a conventional material used for industrial robots for comparison; two resin materials, FELCARBO (Futaba) and MC901; three 3D-printed materials, Onyx (Markforged), Onyx with continuous carbon fiber (CF) (Markforged), and POTICON (Otsuka Chemical).

MC901 is a nylon resin material widely used in engineering and is from bulk material via a cutting process. FELCARBO is a resin material produced by laminating layers of non-woven carbon fibers, high-pressure molding, and cutting. Unlike conventional carbon fiber reinforced plastics (CFRP), FELCARBO is a new lightweight material with high machinability and mechanical properties similar to isotropic materials.

POTICON (NTL34M) is a nylon resin reinforced with potassium titanate fibers. The specimen is fabricated using the Raise 3D Pro2 (Raise 3D) 3D printer. Onyx is a nylon resin reinforced with short carbon fibers, and Onyx + CF is a nylon resin reinforced with continuous carbon fibers. Two parts are fabricated with these materials using X7 (Markforged). The 3D printed parts were fabricated with an infill rate of 37%, a triangular fill structure, eight solid layers, and two walls. The nominal mechanical properties of the above five materials and A5052 with comparative materials are shown in Table. II.

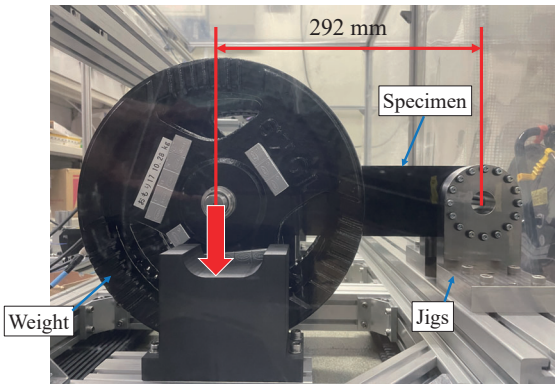

Fig. 2: Load condition of the experiment.

III. Experiment Apparatus

A. Measurement Condition

The creep deformation of resin materials is greatly affected by temperature and load. The temperature in the experiment chamber is set to 25°C, which is the room temperature used for industrial robots. For the load condition, a weight with a mass of 42.08 kg is added at a distance of 292 mm from the fixed part to the tip of the cantilever beam, as shown in Fig. 2. We derive this load condition by assuming that an industrial robot whose maximum reach is 1000 mm picks up a weight of 12.3 kg in a horizontal posture. Under these test conditions, measurements were conducted simultaneously for 1600 hours on specimens of six materials.

B. Mechanical Condition

The fixed end of the specimen is fastened to a fixture jig of SUS304 (shown in Fig. 2) using M4 screws with a fastening torque of 3.6 Nm for the 16 equally-distributed through holes in the specimen. For MC901 and the three 3D printed parts, we apply our previously proposed fastening method [6]. The diameter of the through-holes is 6.2 mm, and thin-walled pipes made of SUS304 with an inner diameter of 4.0 mm and wall thickness of 1.0 mm is inserted into each. A screw is inserted inside the thin-walled pipe to fasten the parts. This fastening method prevents the screws from sinking into the resin part due to the high compressive force applied to the weak resin material. For FELCARBO and A5052, the diameter of the through-holes is set to 4.2 mm and screws

TABLE II: Material properties. [9][10][11][12][13][14][15]
(A large industrial robot link is manufactured by iron casting. FC300 is a typical cast iron. PEEK is a typical high-performance engineering resin and has material property values comparable to nylon's. It has superior performance with significantly less moisture absorption. However, its high heat resistance makes it difficult to use as a 3D printer filament. Both FC300 and PEEK are not used in the experiment and are shown only for comparison.)

Material	FC300	A5052	FELCARBO	MC901	POTICON	Onyx	Onyx+CF	PEEK
Density [g/cm^3]	6.8-7.8	2.7	1.3	1.2	1.3	1.2	1.4	1.3
Tensile strength [MPa]	190-300	260	270	96	100	37	800	100
Tensile modulus [GPa]	92.4	68	22	3.4	5.6	2.4	60	3.8
Bending strength [MPa]	-	-	300	110	167	71	540	163
Bending modulus [GPa]	-	-	18	3.5	6.3	3.0	51	3.5

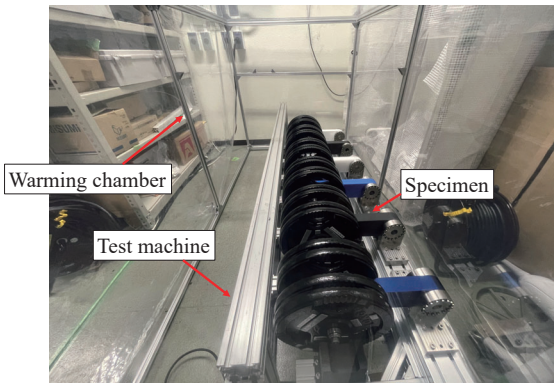

Fig. 3: Experiment apparatus without laser displacement sensors and the temperature control device.

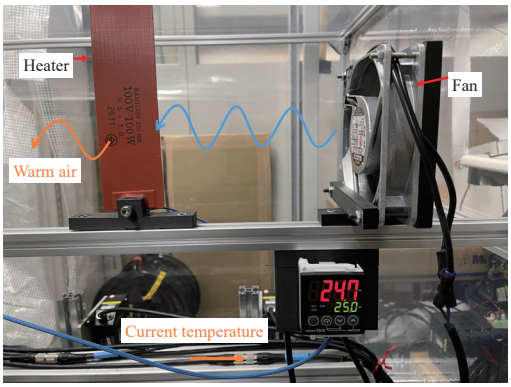

Fig. 4: Temperature control. Warm air is circulated by blowing on a heater whose surface rises to 200°C.

are inserted through them to fasten the parts directly this was done because no deformation was observed when the parts were fastened with a screw in the preliminary experiments.

Then, four weights are each adjusted to 10.52 kg using stick-on weights. A collar is inserted into the weights' center hole to eliminate mechanical play between the weights' inner diameter and the specimen's inner diameter. The 42.08 kg load is assembled by connecting the collar to a shaft made of SUS304. In addition, FINE U-NUT (Fuji Seimitsu) are installed on the ends of the shaft to restrain the weights in the axial direction.

Figure 3 shows the six specimens installed on the experiment apparatus, with the load at the end of each cantilever beam. In order to minimize the difference in test duration and specimen deformation during preparations, jacks are installed to support the weights. These jacks are lowered at the beginning of the experiment and removed from the experiment apparatus.

C. Temperature Management

The temperature setting must be controlled because it affects the creep deformation and can cause measurement errors due to the temperature dependency of the laser displacement transducer used in this study. For this reason, a simplified thermal insulation chamber, as shown in Fig. 3, is installed around the experiment apparatus, and the air conditioning system controls the temperature in the room where the experiment apparatus is installed. The temperature control equipment (shown in Fig. 4) is also installed within the thermal insulation chamber, and temperature control is conducted by circulating warm air inside the chamber while feeding back the temperature obtained by thermocouples installed in the center of the experiment apparatus.

D. Measurement System

We record time series data of the specimens' displacements, temperature in the testing chamber, and temperature of the surface of the laser displacement transducers. The displacement of each specimen is measured using an LK-H150 (KEYENCE) laser displacement meter and logged by an LK-G5000 (KEYENCE). Displacement is measured at

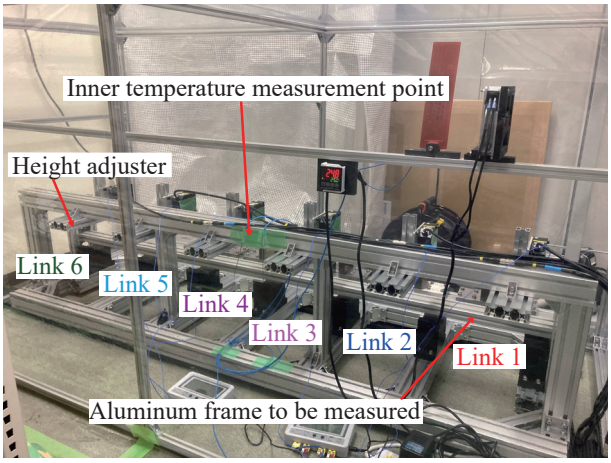

Fig. 5: The configurations of the preliminary experiment. In this experiment, the top of the aluminum frame is aligned with the height of the measurement points in the main experiment.

a chamfered point on the end face of the shaft used to connect the weight to each specimen. The temperature inside the chamber and the temperature of the surface of the laser displacement transducer are measured using a thermocouple installed in the center of the experiment apparatus and a thermocouple attached to the surface of the laser displacement transducer, respectively.

IV. Calibration of the Laser Displacement Meter

As a preliminary experiment, an aluminum frame was fixed across the apparatus instead of the specimens (shown in Fig. 5) so that the displacement would match the initial displacement during the main experiment. The displacement of the top surface of the aluminum frame, the temperature inside the chamber, and the temperature of the surface of the laser displacement meter were acquired as time-series data over the course of four days. Fig. 6 shows the time-series changes in the temperature in the chamber and the temperature of the surface of each laser displacement meter. We confirmed that the temperature fluctuations in the chamber and on the surface of each laser displacement meter was within 0.4°C and 1.7°C respectively, which was a sufficiently negligible deviation. Fig. 7 shows the time-series variation of the displacement obtained by each laser displacement meter. We confirmed that each displacement measurement drifted at a constant rate as time passed. Therefore, the amount of drift per unit of time (shown in Table III) was used to calibrate each laser displacement meter.

V. Measurement Procedure

The measurement procedure is described below.

1) The test specimen is attached the test specimen to the fixture using M4 screws with fastening torque of 3.6 Nm. The fixture is then attached to the main frame of the experiment apparatus.
2) The weights are attached to the tip of the specimen while supporting it with a jack.

TABLE III: Measured displacement drift for calibration.

Link No.	Drift [μm/50hour]
1	6.0
2	4.5
3	3.8
4	4.7
5	2.1
6	6.5

3) The temperature control system is turned on and allowed to stabilize until the temperature inside the chamber at 25°C.
4) The laser displacement meter is turned on and its reading allowed to stabilize over the course of 4 hours.
5) The measurement of thermometer and laser displacement meter are started simultaneously, the jacks supporting the weights are removed, and the measurement for 1600 hours is started.

VI. Results

The righthand figure of Fig. 8 shows the measurement results of the temperature inside the chamber and the temperature on the surface of the laser displacement meter. The temperature deviations were approximately less than 1.5 °C. In the preliminary experiment, the temperature fluctuation suppressed less than 0.7 °C; thus, the temperature changes were much more significant than we expected. This is due to the difference in the outside temperature. The preliminary experiment was conducted in May, and the outside temperature is close to the target temperature. On the other hand, the main experiment was conducted from July to September, where the outside temperature is often 10 °C higher than the target temperature. Although the ambient air temperature in the experiment room was kept at approximately 17 °C by the air conditioner in our building, the temperature control device developed in the experiment apparatus was affected by the outside air conditioning performance because the experiment apparatus did not have a cooling function. There is a strong correlation between the inner and surface temperature of the displacement meter. Thus, we must consider the displacement measurement errors due to temperature fluctuations. We observe irregular temperature changes marked by orange areas numbered (1) and (3). These are due to the unexpected power down of the air conditioning system in our building. We also lost the measurement data in the light blue area (2) and (4) because of the instantaneous power failure of the logging system. We observed small spikes in the light blue area (5) because of an earthquake. Although the experiment encountered the troubles mentioned above, we successfully obtained the primary trend of the creep deformation in the long time range.

The left figure of Fig. 8 shows the displacement measurement results for 1600 hours. The baseline of each displace-

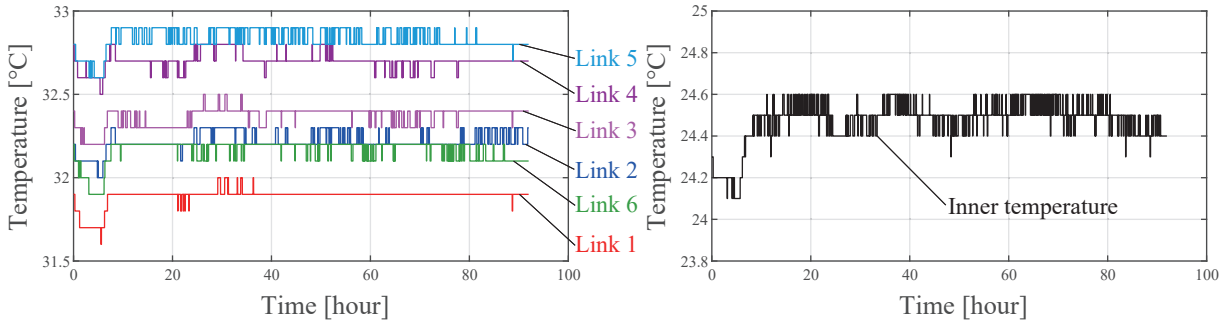

Fig. 6: The temperature measurement result of the preliminary experiments.

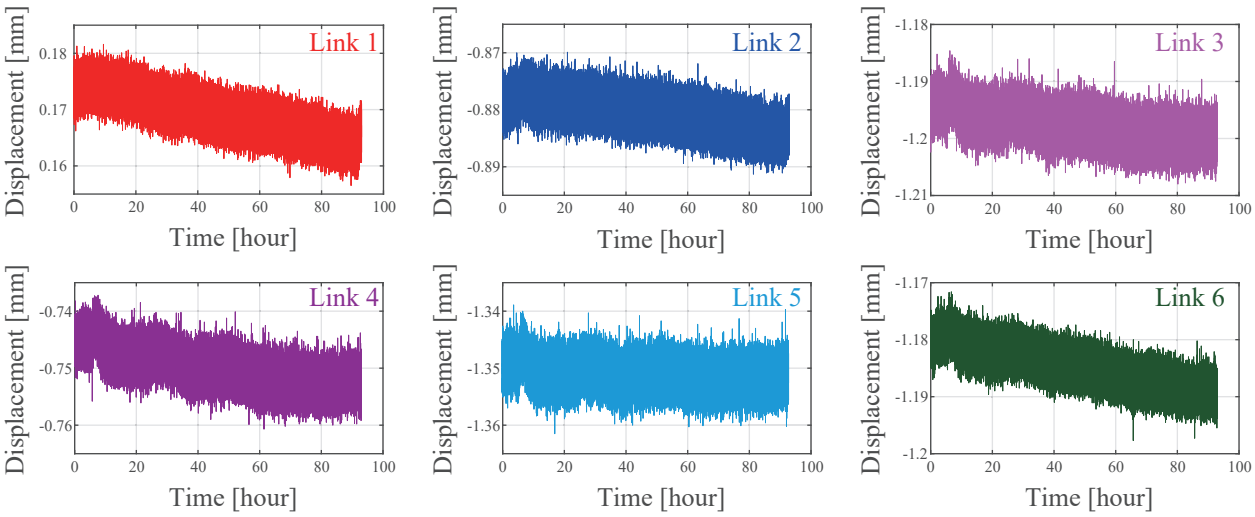

Fig. 7: The displacement result of the preliminary experiments.

ment value was obtained from the measurement value at 5 minutes after removing the jack of the first specimen because removing all jacks took a few minutes.

Negligible small deformation was observed in the time series for A5052, which is consistent with the fact that creep deformation does not occur at room temperature. [1] Furthermore, the time-series deformation of FELCARBO is also small. This indicates that FELCARBO does not have creep deformation under the load and temperature in these conditions, suggesting an excellent candidate to replace the aluminum material if we can afford to use it. (One of the drawbacks of FELCARBO for industrial applications is the material cost and machining process shown in Table I.)

The deformation of MC901 was about 0.2 mm, but the displacement did not significantly change over time after 500 hours, indicating that the creep deformation could be suppressed to 0.2 mm. The deformation of the 3D printed parts, Onyx+CF, POTICON, and Onyx, at 1600 hours was 0.7 mm, 1.7 mm and 3.8 mm, respectively. These values were significantly large compared to MC901, whereas the filaments of these 3D printed materials are made from the same nylon resin material. This is due to the low in-fill rate of 37 % of the 3D-printed specimens. In other words, the 40 kgf load was too large for the 3D printed parts with a 37 % in-fill rate.

As for the comparison with or without the continuous fiber in Onyx, the continuous fiber suppresses the creep deformation. However, we still observe the creep deformation with Onyx + CF that does not agree with the mechanical property of the CF in Table II. This is because of the improper allocation of the CF. The CF is automatically allocated by the slicing (modeling) software “Eiger” supported by Markforged, and the CF is placed on the front/back surface of the specimen shown in Fig.1(c). These surfaces are perpendicular to the load direction and did not contribute much to suppress the creep deformation. The CF allocation in the top/bottom surface of the specimen would significantly decrease the creep deformation.

VII. CONCLUSIONS

In this paper, an experiment apparatus that measures the creep deformation under practical shape and load conditions was fabricated for structural parts of industrial robots. The apparatus measured the creep deformation of two machined bulk resin materials, three 3D printed parts, and conventional

[1]The measured deformation is slightly positive at 1600 hours, which is not physically correct. This is because of the calibration of the laser displacement meter described in Section IV. The calibration was based on the short period of preliminary measurement. Thus, the measurement results shown here include approximately ±0.05 mm errors.

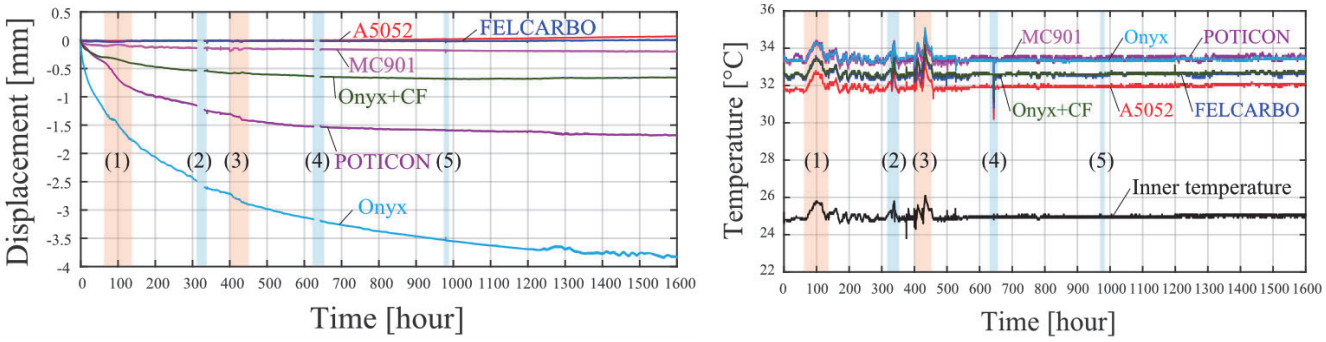

Fig. 8: The result of the creep deformation of the links. (left) the result of displacement, (right) the result of temperature.

aluminum alloy A5052. Almost no creep deformation was observed in FELCARBO under the test conditions of the two bulk materials. The creep deformation was observed in MC901, and the deformation settled after approximately 500 hours. The creep deformation continued in all 3D-printed parts, which was significant compared to A5052, FELCARBO, and MC901.

As for future work, structural improvements are necessary for 3D printed parts, such as modification of the in-fill rate, filling structure, optimum allocation of the reinforcement fibers, and the shape of the structural parts to suppress creep deformation. This paper measured simple shape structure and single load condition. It is necessary to clarify the specifications of applicable industrial robots for each material in the future by conducting measurements under various loading conditions with the more practical shape of structures. Additionally, the problem of heat dissipation of the actuator is also crucial for using thermoplastic materials in industrial robots. Materials with high heat transfer coefficients should be considered in the future.

ACKNOWLEDGMENT

This research is subsidized by New Energy and Industrial Technology Development Organization (NEDO) under a project JPNP20016. This paper is one of the achievements of joint research with and is jointly owned copyrighted material of ROBOT Industrial Basic Technology Collaborative Innovation Partnership.

We thank Prof. Naoyuki Takesue (Tokyo Metropolitan University), Prof. Yusuke Ohta (Chiba Institute of Technology), and Prof. Takeshi Takaki (Hiroshima University) for their valuable comments and discussion.

REFERENCES

[1] Sallam A. Kouritem and Mohammed I. Abouheaf and Nabil Nahas and Mohamed Hassan, "A multi-objective optimization design of industrial robot arms," Alexandria Engineering Journal, Vol. 61, No. 12, pp.12847-12867, 2022, DOI: 10.1016/j.aej.2022.06.052

[2] Mustafa Bugday and Mehmet Karali, "Design optimization of industrial robot arm to minimize redundant weight," Engineering Science and Technology, an International Journal, Vol. 22, No. 1, pp. 346-352, 2019, DOI: 10.1016/j.jestch.2018.11.009.

[3] Rodrguez, Jos F, Thomas, James P, and Renaud, John E, "Mechanical behavior of acrylonitrile butadiene styrene fused deposition materials modeling," Rapid Prototyping Journal, Vol. 9, No. 4, pp. 219-230, 2003, DOI: 10.1108/13552540310489604.

[4] Takaki, Takeshi and Kanekiyo, Masahito and Endo, Gen, "Damping Characteristics in Adaptation of Plastics for Robot Structures," International Symposium on System Integration (SII), pp. 1-4, 2023, DOI: 10.1109/SII55687.2023.10039233.

[5] Takesue, Naoyuki and Ode, Yuri, "Stiffness Model of Single-Geared Joint with 3D-Printed Link in Robot Arm," International Symposium on System Integration (SII), pp. 1-6, 2023, DOI: 10.1109/SII55687.2023.10039160.

[6] Endo, Gen and Tsukamoto, Yuta and Nabae, Hiroyuki and Takaki, Takeshi, "Proposal of a Fastening Method for Deformable Plastic Parts and Rigid Metal Parts," International Symposium on System Integration (SII), pp. 1-6, 2023, DOI: 10.1109/SII55687.2023.10039451.

[7] Mohammad Reza Adibeig and Farid Vakili-Tahami and Mohammad-Ali Saeimi-Sadigh, "Numerical and experimental investigation on creep response of 3D printed Polylactic acid (PLA) samples. Part I: The effect of building direction and unidirectional raster orientation," Journal of the Mechanical Behavior of Biomedical Materials, Vol. 145, pp. 106025, 2023, DOI: 10.1016/j.jmbbm.2023.106025.

[8] Zhang Hanyin, Cai Linlin, Golub Michael, Zhang Yi, Yang Xuehui, Schlarman Kate, and Zhang Jing, "Tensile, Creep, and Fatigue Behaviors of 3D-Printed Acrylonitrile Butadiene Styrene," Journal of Materials Engineering and Performance, Vol. 27, pp. 57-62, 2018, DOI: 10.1007/s11665-017-2961-7.

[9] (2023, Oct.) JIS G5501 FC300 Gray Cast Iron. [Online]. Available: https://www.iron-foundry.com/JIS-G5501-FC300-gray-cast-iron.html

[10] (2023, Aug.) Kabuku Connect, A5052. [Online]. Available: https://www.kabuku.io/guide/metal/aluminum/a5052/

[11] (2023, Aug.) Futaba, FELCARBO. [Online]. Available: https://www.cfrp.mtb.futaba.co.jp/felcarbo

[12] (2023, Aug.) Hirosugi, MC. [Online]. Available: https://hirosugi.co.jp/technical/material/MC.html

[13] (2023, Aug.) Markforged, Onyx. [Online]. Available: https://markforged.com/jp/materials/plastics/onyx

[14] (2023, Aug.) Raise 3D, TDS. [Online]. Available: https://raise3d.jp/download#download05

[15] (2023, Oct.) PEEK Shapes Typical Data. [Online]. Available: https://www.junhuapeek.com/PEEK-Shapes-pl3160579.html?gclid=Cj0KCQjw1aOpBhCOARIsACXYv-eTcX9-LkJeSEWSJmbjnh8tjBCUCkWYFEMztAvvFLEADuMfUIrWSXIaAlxKEALw_wcB